Journal of Organometallic Chemistry 737 (2013) 40–46

Contents lists available at SciVerse ScienceDirect

Journal of Organometallic Chemistry

journal homepage: www.elsevier.com/locate/jorganchem

Cis configured bis phosphine platinum(II) chalcogenolate complexes: Structures, NMR and computational studies

Rohit Singh Chauhan [a], G. Kedarnath [a], A. Wadawale [a], D.K. Maity [b], James A. Golen [c], Arnold L. Rheingold [c], Vimal K. Jain [a,*]

[a] *Chemistry Division, Bhabha Atomic Research Centre, Trombay, Mumbai 400 085, India*
[b] *Theoretical Chemistry Section, Bhabha Atomic Research Centre, Trombay, Mumbai 400 085, India*
[c] *Department of Chemistry and Biochemistry, University of California, San Diego, La Jolla, CA 92093-0358, United States*

ARTICLE INFO

Article history:
Received 7 January 2013
Received in revised form
6 March 2013
Accepted 13 March 2013

Keywords:
Platinum
Selenolate
Tellurolate
NMR
X-ray
Density functional calculation

ABSTRACT

Reactions of $[PtCl_2(P^\cap P)]$ ($P^\cap P$ = dppm, dppe or dppp) with $Pb(SMes)_2$ and sodium arylchalcogenolates yielded mononuclear complexes of the type, *cis*-$[Pt(EAr)_2(P^\cap P)]$ [EAr = EMes (E = S, Se or Te; Mes = mesityl), Sepym (pym = 2-pyrimidyl) or SepymMe$_2$ (pymMe$_2$ = 4,6-dimethyl-2-pyrimidyl]. These complexes were characterized by elemental analyses and NMR (^1H, ^{31}P) spectroscopy. The molecular structures of $[Pt(SeMes)_2(dppp)]\cdot½C_6H_6$, $[Pt(TeMes)_2(dppp)]\cdot 3C_6H_6$, $[Pt(SeC_4H_3N_2)_2(dppm)]$ and $[Pt\{SeC_4H(4,6\text{-}Me_2)N_2\}_2(dppm)]\cdot CH_2Cl_2$ were established by single crystal X-ray diffraction analyses. An attempt has been made to rationalize the NMR data with the nature of chelated bis phosphine ligand, chalcogen atom and aryl substituent on the chalcogen atom. The energy difference (ΔE), calculated by DFT, is very small between various conformers. The calculated ΔE between various conformers of mesitylthiolate dppp complex lies in the range of 0.1–1.0 kcal/mol; the same for mesitylselenolate complex lies in the range of 0.5–2.2 kcal/mol and for mesityltellurolate complex it is in the range of 1.0–3.0 kcal/mol.

1. Introduction

Mononuclear *cis* configured palladium and platinum organochalcogenolate complexes, *cis*-$[M(ER')_2(PR_3)_2]$ are of considerable interest as they are used as molecular tectons for constructing a variety of bi- and high-nuclearity complexes [1–3] and are believed to be catalytically active species in metal catalyzed C–E (E = S or Se) bond formation [4,5]. In the case of monodentate ER′ and PR_3 ligands, isomerization to the thermodynamically more stable trans form [6] and polymerization to R′E-bridged species [7] are usually encountered. To circumvent these problems, chelating phosphines [8,9], and/or chelating [10,11]/bulky [11] chalcogenolate ligands are employed. The aryl groups on chalcogenolate ligands can mutually adopt different orientations with respect to the metal square plane, *viz.*, *anti* form (A), *syn* form (B), aryl-rings coplanar with the metal plane (C) and aryl planes perpendicular to metal plane (D) (Scheme 1). In general distortions from these idealized conformations are usually encountered in the solid state (from X-ray crystallography). The two Pt–E distances in *cis*-$Pt(EAr)_2(P^\cap P)$ are often nonequivalent as a consequence the two Pt–P distances are also differing slightly from each other, although complexes with the same two Pt–E distances are also reported. The difference in the two Pt–E distances, irrespective of the nature of chalcogen atom, can be as large as 0.07 Å (Supplementary material). Such differences are, however, not evident from the ^{31}P and ^{195}Pt NMR spectra in solution and are indicative of equivalence of the two ^{31}P nuclei.

In the light of the above and to gain further insight on the structural features of *cis*-$[Pt(EAr)_2(P^\cap P)]$ complexes, we have chosen a sterically hindered Ar (mesityl) as well as heterocyclic group containing nitrogen atoms (*e.g.*, pyrimidyl). The latter small bite heterocyclic chalcogenolate ligand shows several binding possibilities (viz. terminal E bonding, E-bridging, N,E-chelating, N,E-bridging, N,E-chelating-cum-E bridging or N,E-bridging-cum-E-bridging modes (E = S, Se, Te)) [12,13]. The complexes with higher homologues (Se, Te) quite often show remarkable differences in reactivity than the corresponding thio derivatives [14–16]. Furthermore, the tellurolate complexes are scantly investigated. Results of this work are reported herein.

2. Experimental

The compounds $[PtCl_2(P^\cap P)]$ [$P^\cap P$ = dppm (bis(diphenylphosphino)methane), dppe (1,2-bis(diphenylphosphino)ethane), dppp (1,3-bis(diphenylphosphino)propane)] [17] and the ligand precursors

---

[*] Corresponding author. Tel.: +91 22 25595095; fax: +91 22 25505151.
E-mail addresses: arheingold@ucsd.edu (J.A. Golen), jainvk@barc.gov.in (V.K. Jain).

0022-328X/$ – see front matter © 2013 Elsevier B.V. All rights reserved.
http://dx.doi.org/10.1016/j.jorganchem.2013.03.030

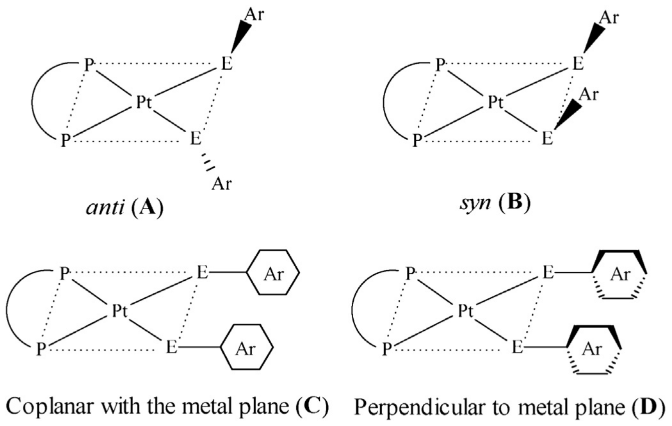

Scheme 1.

$(SeMes)_2$ [18], $(TeMes)_2$ [19], $(SeC_4H_3N_2)_2$, $\{SeC_4H(4,6\text{-}Me)_2N_2\}_2$ [16] and $[Pb(SMes)_2]$ [20] were prepared by literature methods. All reactions were carried out under a nitrogen atmosphere in dry and distilled analytical grade solvents at room temperature. The ^1H and $^{31}P\{^1H\}$ NMR spectra were recorded on a Bruker Avance-II spectrometer operating at 300 and 121.49 MHz, respectively. Chemical shifts are relative to internal chloroform (d 7.26) for ^1H, external 85% H_3PO_4 for ^{31}P. Elemental analyses were carried out on a Thermo Fischer Flash EA1112 CHNS analyzer.

Intensity data for $[Pt(SeMes)_2(dppp)]\cdot½C_6H_6$, $[Pt(TeMes)_2(dppp)]\cdot3C_6H_6$, $[Pt(SeC_4H_3N_2)_2(dppm)]$ and $[Pt\{SeC_4H(4,6\text{-}Me_2)N_2\}_2(dppm)]\cdot CH_2Cl_2$ were measured on a Bruker Apex-II, CCD diffractometer with Mo-K$_\alpha$ radiation so that $\theta_{max} = 27.5°$. The structures were solved by direct methods [21] and refinement was on F^2 using data that had been corrected for absorption effects with an empirical procedure. Non-hydrogen atoms were modelled with anisotropic displacement parameters, hydrogen atoms in their calculated positions. Molecular structures were drawn using ORTEP [22]. Crystallographic and structural determination data are listed in Table 1.

Full geometry optimization of mesityl chalcogenolate (S, Se and Te) complexes of platinum has been carried out by applying a DFT functional, namely, BP86. The BP86 is a generalized gradient approximation (GGA) functional that combines Becke's 1988 exchange functional with Perdew's 1986 correlation functional. SARC-ZORA basis sets for platinum, Gaussian type atomic basis functions, 6-31G(d) for H, C, P, S and Se atoms and 3-21G for Te atom are applied for all the calculations. Basis sets for Pt and Se atoms were obtained from Extensible Computational Chemistry Environment Basis Set Database, Pacific Northwest National Laboratory [23]. The quasi-Newton–Raphson based algorithm has been applied to carry out geometry optimization to locate the minimum energy structure in each case. All these calculations have been carried out applying GAMESS suit of *ab initio* programs on a LINUX cluster platform [24].

2.1. Syntheses of complexes

2.1.1. $[Pt(SMes)_2(dppm)]$

To a benzene suspension of $[PtCl_2(dppm)]$ (100 mg, 0.15 mmol) was added a dichloromethane solution of $[Pb(SMes)_2]$ (82 mg, 0.16 mmol) with stirring which continued for 6 h at room temperature whereupon a yellow turbid solution was formed. The latter was centrifuged and passed through Celite and the filtrate was concentrated under reduced pressure. The residue was extracted with dichloromethane, filtered and passed through a Florisil column. Hexane was added to the resulting solution to give a yellow powder (yield 81 mg, 60%). Similarly $[Pt(SMes)_2(dppe)]$ and $[Pt(SMes)_2(dppp)]$ were prepared. Pertinent data are given in Table 2.

2.1.2. $[Pt(SeMes)_2(dppm)]$

To a benzene suspension (15 cm^3) of $[PtCl_2(dppm)]$ (120 mg, 0.18 mmol) was added a methanol–benzene solution (10 cm^3) of NaSeMes [prepared from $(SeMes)_2$ (80 mg, 0.20 mmol) in benzene

Table 1
Crystallographic and structural determination data for $[Pt(SeMes)_2(dppp)]\cdot½C_6H_6$, $[Pt(TeMes)_2(dppp)]\cdot3C_6H_6$, $[Pt(SeC_4H_3N_2)_2(dppm)]$, $[Pt\{SeC_5H(4,6\text{-}Me)N_2\}_2(dppm)]\cdot CH_2Cl_2$.

Complex	$[Pt(SeMes)_2(dppp)]\cdot½C_6H_6$	$[Pt(TeMes)_2(dppp)]\cdot3C_6H_6$	$[Pt(SeC_4H_3N_2)_2(dppm)]$	$[Pt\{SeC_5H(4,6\text{-}Me)_2N_2\}_2(dppm)].CH_2Cl_2$
Chemical formula	$C_{45}H_{48}P_2PtSe_2\cdot½C_6H_6$	$C_{45}H_{48}P_2PtTe_2\cdot3C_6H_6$	$C_{33}H_{28}N_4P_2PtSe_2$	$C_{37}H_{36}N_4P_2Pt\,Se_2\cdot CH_2Cl_2$
Formula wt.	1042.84	1335.39	895.54	1036.57
Crystal size (mm^3)	0.40 × 0.30 × 0.20	0.38 × 0.33 × 0.30	0.20 × 0.15 × 0.10	0.15 × 0.10 × 0.10
Radiation used for data collection	Mo-K$_\alpha$	Mo-K$_\alpha$	Mo-K$_\alpha$	Mo-K$_\alpha$
Crystal system	Monoclinic	Orthorhombic	Monoclinic	Orthorhombic
Space group	$P2_1/n$	$Pbcn$	$C2/c$	$Pna2_1$
Unit cell dimensions				
a (Å)	14.000(5)	20.927(3)	48.245(2)	15.8773(4)
b (Å)	22.376(7)	12.8611(16)	8.8359(4)	14.4948(4)
c (Å)	13.583(8)	20.875(3)	22.1322(10)	16.7069(5)
α (°)	90	90	90	90
β (°)	98.25(4)	90	96.990(2)	90
γ (°)	90	90	90	90
Volume (Å^3)	4211(3)	5618.3(12)	9364.6(7)	3844.90(18)
Z	4	4	12	4
ρ_{calcd}, g cm^{-3}	1.645	1.578	1.901	1.791
θ for data collection (°)	2.67–28.33	1.86–25.37	1.70–25.44	2.57–25.85
μ (mm^{-1})/F(000)	5.170/2060	3.610/2620	6.960/5160	5.798/2016
Index range	$-10 \le h \le 18$	$-24 \le h \le 25$	$-58 \le h \le 57$	$-19 \le h \le 19$
	$0 \le k \le 29$	$-15 \le k \le 15$	$-10 \le k \le 10$	$-17 \le k \le 13$
	$-17 \le l \le 17$	$-25 \le l \le 25$	$-26 \le l \le 26$	$-20 \le l \le 20$
No of reflections collected	11,879	40,961	61,532	28,372
No of independent reflection/no. of observed reflections with $I > 2\sigma I$	9922/4457	5156/4527	8678/7319	7412/6610
Data/restraints/parameters	9922/0/484	5156/0/308	8678/0/569	7412/1/447
Final R_1, ωR_2 indices	0.0474/0.0905	0.0212/0.0474	0.0264/0.0495	0.0250/0.0513
R_1, ωR_2 (all data)	0.1702/0.1211	0.0273/0.0509	0.0375/0.0523	0.0329/0.0538
Goodness of fit on F^2	0.932	1.042	1.038	1.042

Table 2
Physical, analytical and NMR data for [Pt(EAr)$_2$(P$^\cap$P)].

Complex	Recrystallization solvent (% yield)	M.p. (°C)	% Analysis: found (calcd.)			NMR data	
			C	H	S or N	^{1}H NMR (δ in ppm)	^{31}P{^{1}H} NMR δ (^1J(Pt–P) in Hz)
[Pt(SMes)$_2$(dppm)]	CH$_2$Cl$_2$–hexane (60)	172	58.12 (58.55)	5.23 (5.03)	7.71 (7.27)	2.03 (s, Me, 3H), 2.40 (s, Me, 6H), 4.18 (t, PCH$_2$), 6.28 (s, Mes), 7.31–7.51 (m), 7.92 (m)[Ph]	−46.4 (2641)
[Pt(SeMes)$_2$(dppm)]	CH$_2$Cl$_2$–hexane (58)	197	53.01 (52.93)	4.83 (4.55)	–	2.03 (s, 4-Me), 2.23 (d, 9.6 Hz, –CH$_2$), 2.40 (s, 2,6-Me), 6.28 (s, 3,5-H), 7.28–7.31 (m, Ph), 7.40–7.49 (m, Ph)	−52.5 (2522)
[Pt(TeMes)$_2$(dppm)]	Benzene–diethyl ether (42)	181	48.62 (48.13)	4.44 (4.13)	–	2.03 (s, 4-Me), 2.17 (d, 0.9 Hz, –CH$_2$), 2.22 (s, 2,6-Me), 6.46 (s, 3,5-H), 7.31–7.36 (m, Ph), 7.39–7.48 (m, Ph), 7.66 (m, Ph), 7.82–7.86 (m)	−57.4 (2422)
[Pt(SeC$_4$H$_3$N$_2$)$_2$(dppm)]	CH$_2$Cl$_2$–hexane (67)	144	44.38 (44.25)	3.15 (3.15)	6.11 (6.25)		−50.8 (2770)
[Pt{SeC$_4$H(4,6-Me$_2$)N$_2$}$_2$(dppm)]	CH$_2$Cl$_2$–hexane (74)	127	46.84 (46.69)	3.88 (3.81)	5.91 (5.89)	1.86 (s, Me), 4.46 (br, PCH$_2$), 6.17 (s, pym), 7.35 (br), 7.93 (br) [Ph]	−49.9 (2685)
[Pt(SMes)$_2$(dppe)]	CH$_2$Cl$_2$–hexane (64)	179	58.34 (58.98)	5.03 (5.17)	7.01 (7.15)	2.07 (s, 4-Me), 2.15 (s, 2,6-Me), 2.23–2.51 (m, –CH$_2$), 6.39 (s, 3,5-H), 7.34–7.43 (m, Ph), 7.63–7.70 (m, Ph)	42.3 (2677)
[Pt(SeMes)$_2$(dppe)]	CH$_2$Cl$_2$–diethyl ether (62)	124	52.66 (53.39)	4.52 (4.68)	–	–	43.8 (2935)
[Pt(TeMes)$_2$(dppe)]	Acetone–diethyl ether (51)	178	48.38 (48.61)	4.31 (4.27)	–	2.18 (s, 4-Me), 2.22–2.31 (m, –CH$_2$), 2.34 (s, 2,6-Me), 6.28 (s, 3,5-H), 7.38–7.41 (m, Ph), 7.79–7.86 (m, Ph).	47.9 (2810)
[Pt(SMes)$_2$(dppp)]	Acetone–hexane (54)	161	59.21 (59.39)	5.43 (5.31)	6.89 (7.04)	2.09 (s, Me), 2.33 (m, -PCH$_2$), 2.48 (br, –CH$_2$), 6.37 (s, 3,5-H), 7.32–7.38 (m, Ph), 7.74 (br, Ph)	−2.9 (2743)
[Pt(SeMes)$_2$(dppp)]	CH$_2$Cl$_2$–hexane (69)	168	54.09 (53.84)	4.66 (4.82)	–	2.10 (s, Me), 2.46 (br, –CH$_2$), 6.45 (s, 3,5-H), 7.30–7.37 (m, Ph), 7.73 (br, Ph).	−6.6 (2775)
[Pt(TeMes)$_2$(dppp)]	Benzene–diethylether (58)	132	49.21 (49.08)	4.37 (4.39)	–	2.17 (s, 4-Me), 2.22–2.42 (m, –CH$_2$), 2.57 (s, 2,6-Me), 6.78 (s, 3,5-H), 7.39–7.59 (m, Ph), 7.75–7.81 (m, Ph).	−6.8 (2469)

and NaBH$_4$ (16 mg, 0.42 mmol) in methanol]. The mixture was stirred for 4 h, whereupon a clear yellow solution was obtained. The solvents were evaporated under reduced pressure. The residue was washed with hexane followed by diethyl ether. The product was extracted with dichloromethane and passed through a Florisil column which on slow evaporation gave yellow crystals of [Pt(SeMes)$_2$(dppm)]. Similarly all other selenolate complexes were prepared.

2.1.3. *[Pt(TeMes)$_2$(dppm)]*

To a benzene suspension (10 cm^3) of [PtCl$_2$(dppm)] (125 mg, 0.19 mmol) was added a methanol–benzene solution (10 cm^3) of NaTeMes [freshly prepared from (TeMes)$_2$ (94 mg, 0.19 mmol) in benzene and NaBH$_4$ (15 mg, 0.40 mmol) in methanol]. The reactants were stirred for 5 h at room temperature to give a red solution. The solvents were removed under vacuum and the residue was washed with diethyl ether and dried under reduced pressure. The product was extracted with benzene, filtered and passed through a Florisil column. The resulting solution was concentrated (5 cm^3) under vacuum which on slow evaporation at room temperature gave red crystals (yield 86 mg, 42%). Similarly all other tellurolate complexes were prepared.

Table 3
Selected bond lengths (Å) and angles (°) of [Pt(SeMes)$_2$(dppp)]·½C$_6$H$_6$.

Pt1–P1	2.246(2)	Pt1–P2	2.238(2)
Pt1–Se1	2.4251(11)	Pt1–Se1	2.4353(13)
Se1–C1	1.887(9)	Se2–C10	1.914(8)
P1–Pt1–P2	97.14(9)	Se1–Pt1–Se2	88.65(4)
P1–Pt1–Se1	85.18(7)	P2–Pt1–Se1	159.95(7)
P1–Pt1–Se2	161.68(7)	P2–Pt1–Se2	94.56(7)
C1–Se1–Pt1	111.0(3)	C10–Pt1–Se2	113.4(2)
P1–Pt1–Se1–C1	−164.5(3)	P2–Pt1–Se1–C1	97.9(4)
P1–Pt1–Se2–C10	−89.4(4)	P2–Pt–Se2–C10	40.2(3)
C1–Se1–Pt1–Se2	−1.7(3)	C10–Se2–Pt1–Se1	−159.7(3)

3. Results and discussion

3.1. *Synthesis and spectroscopy*

Reactions of PtCl$_2$(P$^\cap$P) with either Pb(SMes)$_2$ or 2 equiv of NaEAr (E = Se or Te) (prepared by reductive cleavage of E–E bond in Ar$_2$E$_2$ by NaBH$_4$ in methanol–benzene) gave mononuclear platinum chalcogenolate complexes, [Pt(EAr)$_2$(P$^\cap$P)] [EAr = EMes

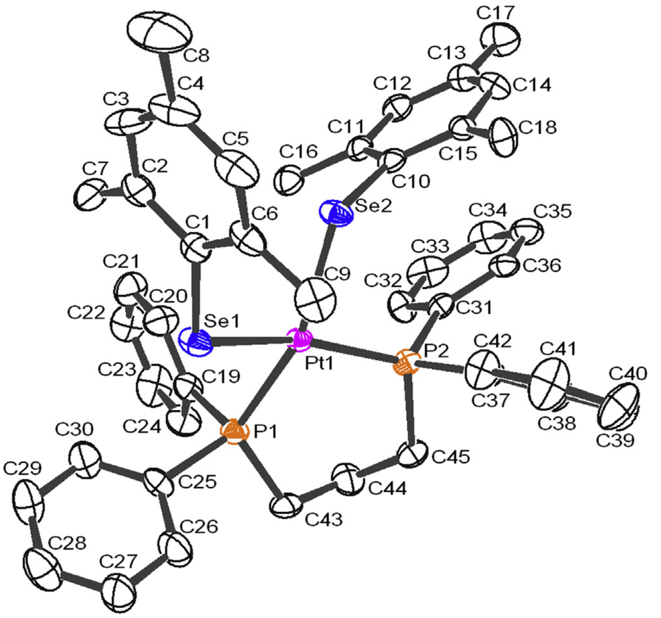

Fig. 1. ORTEP drawing of [Pt(SeMes)$_2$(dppp)]·½C$_6$H$_6$ with atomic number scheme. Hydrogen atoms and the solvent molecule are omitted for clarity.

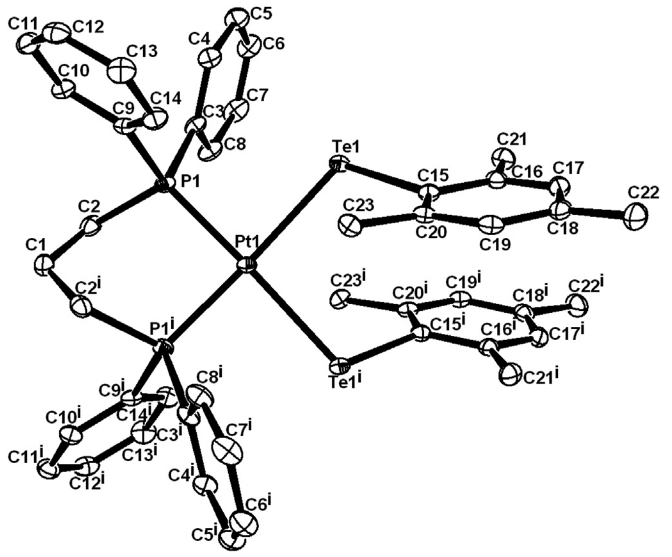

Fig. 2. ORTEP drawing of $[Pt(TeMes)_2(dppp)]\cdot 3C_6H_6$ with atomic number scheme. Hydrogen atoms and the solvent molecule are omitted for clarity.

(E = S, Se or Te; Mes = mesityl), Sepym (pym = 2-pyrimidyl) or $SepymMe_2$ ($pymMe_2$ = 4,6-dimethyl-2-pyrimidyl); $P^{\cap}P$ = dppm, dppe or dppp] as yellow crystalline solids. The reactions with lead mesitylthiolate are quite facile affording desired products in fairly good yield.

The $^{31}P\{^1H\}$ NMR spectra of these complexes displayed single resonances which appeared in the expected range of the respective chelating phosphine complexes of platinum [25]. The resonances were flanked by ^{195}Pt couplings. The magnitude of $^1J(Pt–P)$ lies in the range 2419–3090 Hz and depends on the nature of the chelating phosphine ligand, chalcogen atom and to a some extent on the nature of Ar group on chalcogen. The observed magnitude of $^1J(Pt–P)$ is reduced significantly as compared to the values for the corresponding $[PtCl_2(P^{\cap}P)]$ indicating strong trans influence of the organochalcogenolate ligand. The X-ray structural analysis of $[Pt(SeMes)_2(dppp)]$ reveals that the complex has slightly different two Pt–P and two Pt–Se distances (Table 3). However such differences are not evident from NMR data. The ^{31}P NMR spectrum of this complex in CD_2Cl_2 solution at 700 MHz did not show any noticeable change down to −45 °C.

As is evident from Table 2, the order of coupling constant for each chalcogen atom of EAr group follows the trend dppm < dppp < dppe. The observed trend of coupling is in conformity with the earlier reports [8,25,26]. On keeping the bis phosphine ligand fixed, the coupling constant followed the trend Se > S ≥ Te. Interestingly the π-acidity (nucleophilicity) of chalcogenolate ligand follows the sequence Te > Se ≫ S. The variation of group on chalcogen atom resulted into a slight change in coupling constant (less than 150 Hz) (Supplementary material). Attempts to correlate these values with respect to the nature of Ar group (electronic effect) were inconclusive as the contributions from steric effect of different Ar groups could not be rationalized.

3.2. *Crystal structures*

Molecular structures of $[Pt(SeMes)_2(dppp)]\cdot ½C_6H_6$, $[Pt(TeMes)_2(dppp)]\cdot 3C_6H_6$, $[Pt(SeC_4H_3N_2)_2(dppm)]$ and $[Pt\{SeC_4H(4,6\text{-}Me_2)N\}_2(dppm)]\cdot CH_2Cl_2$ were established by single crystal X-ray diffraction analyses. ORTEP drawings with atomic numbering scheme are depicted in Figs. 1–4 while selected inter-atomic parameters are given in Tables 3–6. Except $[Pt(SeC_4H_3N_2)_2(dppm)]$, these complexes crystallized with the solvent of crystallization. There are two independent molecules of $[Pt(SeC_4H_3N_2)_2(dppm)]$ in the crystal lattice which differ slightly in inter-atomic parameters from each other. The other complexes comprised of discrete monomeric units.

The platinum atom in these complexes adopts a distorted square planar geometry defined by two chalcogenolate ligands and the chelating phosphine ligand in a *cis* configuration. The Pt–Se (2.4182(5)–2.4914(5) Å), Pt–Te (2.6394(3) Å) and Pt–P (2.238(2)–2.2710(8) Å) distances can be compared with mononuclear platinum chalcogenolate complexes, $[Pt(EAr)_2(P^{\cap}P)]$ (E = Se or Te) [8,11,27,28]. The two Pt–Te distances in $[Pt(TeMes)_2(dppp)]\cdot 3C_6H_6$ are essentially the same, whereas these are distinctly different in $[Pt(TePh)_2(dppe)]$ (Pt–Te = 2.6465(7), 2.6053(6) Å) [28] and $[Pt(TeTh)_2(dppe)]$ (Pt–Te = 2.6594(9), 2.607(1) Å) [28].

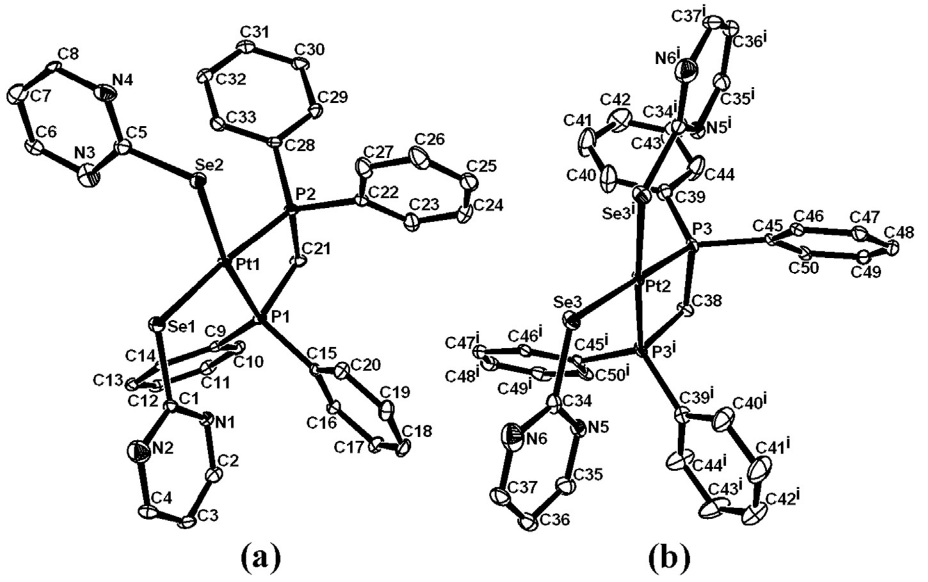

Fig. 3. ORTEP drawing of $[Pt(SeC_4H_3N_2)_2(dppm)]$ with atomic number scheme.

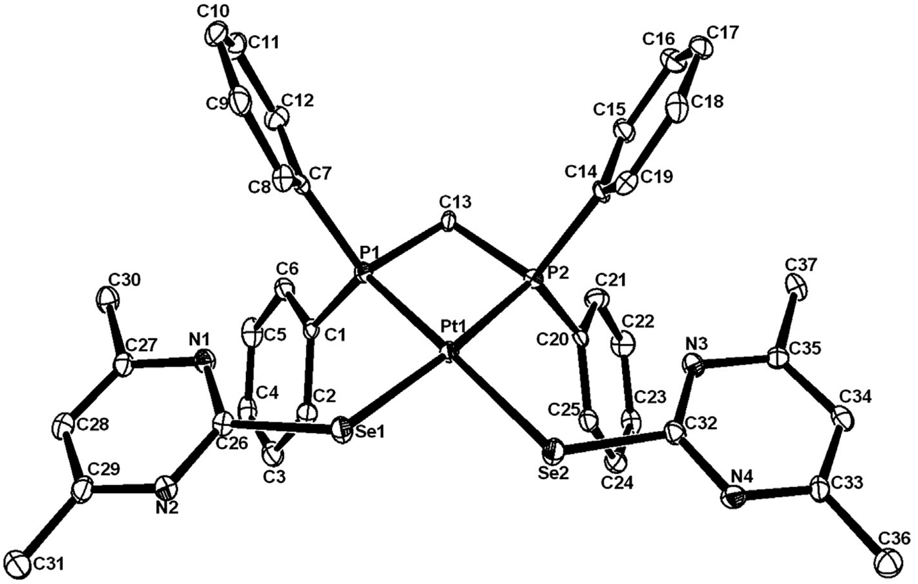

Fig. 4. ORTEP drawing of [Pt{SeC$_4$H(4,6-Me$_2$)N$_2$}$_2$(dppm)]·CH$_2$Cl$_2$ with atomic number scheme. Hydrogen atoms and the solvent molecule are omitted for clarity.

The Pt–P distance in [Pt(TeMes)$_2$(dppp)]·3C$_6$H$_6$ (2.2710(8) Å) is marginally longer than the selenium analogue, [Pt(SeMes)$_2$(dppp)]·½C$_6$H$_6$ (av. 2.242 Å) indicating stronger *trans* influence of the tellurolate group. The E–Pt–E angle in these complexes lies in the range 79.633(17)°–94.673 (13)°. The E–M–E angle in *cis*-[M(EAr)$_2$(PR$_3$)$_2$] (M = Pd or Pt; E = S, Se, Te) complexes varies between 78° and 101° [8,9,11,27,28] and is influenced by the orientation of the aryl group on the chalcogen atom with respect to the M–E bond [28].

Table 4
Selected bond lengths (Å) and angles (°) of [Pt(TeMes)$_2$(dppp)]·3C$_6$H$_6$.

Pt1–P1	2.2710(8)	Te1–C15	2.141(3)
Pt1–Te1	2.6394(3)		
P1–Pt1–P1	91.17(4)	Te1–Pt1–Te1	94.673(13)
P1–Pt1–Te1	169.734(19)	C15–Te1–Pt1	108.15(8)
P1–Pt1–Te1	87.97 (2)		
P1–Pt1–Te1–C15	152.40(8)	C15–Te1–Pt1–Te1′	−37.54(8)
P1–Pt1–Te1′–C15′	67.03(14)		

Table 5
Selected bond lengths (Å) and angles (°) of [Pt(SeC$_4$H$_3$N$_2$)$_2$(dppm)].

Molecule **a**		Molecule **b**	
Pt1–P1	2.2642(10)	Pt2–P3	2.2603(11)
Pt1–P2	2.2488(11)	Pt2–Se3	2.4537(5)
Pt1–Se1	2.4182(5)	Se3–C34	1.908(5)
Pt1–Se2	2.4914(5)		
Se1–C1	1.903(4)		
Se2–C5	1.920(5)		
P1–Pt1–P2	73.85(4)	P3–Pt2–P3′	74.09(6)
P1–Pt1–Se1	104.83(3)	P3–Pt2–Se3	176.25(4)
P1–Pt1–Se2	169.50(3)	P3–Pt2–Se3′	102.86(3)
P2–Pt1–Se1	175.11(3)	Se3–Pt2–Se3′	80.27(2)
P2–Pt1–Se2	95.67(3)	C34–Se3–Pt2	111.71(14)
Se1–Pt1–Se2	85.559(16)		
C1–Se1–Pt1	110.62(13)		
C5–Se2–Pt1	106.96(13)		
P1–Pt1–Se1–C1	15.01(14)	P3–Pt2–Se3–C34	8.82(15)
P1–Pt1–Se2–C5	106.2(2)	C34–Se3–Pt2–Se3′	−169.08(15)
P2–Pt1–Se1–C1	−58.7(4)	C34–Se3–Pt2–P3	44.1(5)
P2–Pt1–Se2–C5	102.60(14)		
C1–Se1–Pt1–Se2	−163.41(13)		
C5–Se2–Pt1–Se1	−82.10(14)		

Each of the two Pt–Se and two Pt–P distances, except molecule **b** of [Pt(SeC$_4$H$_3$N$_2$)$_2$(dppm)] are distinctly different in selenolate complexes while in molecule **b** of [Pt(SeC$_4$H$_3$N$_2$)$_2$(dppm)] the two Pt–Se and Pt–P distances are the same. The P–Pt–P and Se–Pt–Se angles in [Pt(SeC$_4$H$_3$N$_2$)$_2$(dppm)] [73.85(4)°, 85.559(16)° (molecule **a**) and 74.09(6)°, 80.27(2)° (molecule **b**)] and [Pt{SeC$_4$H(4,6-Me$_2$)N}$_2$(dppm)]·CH$_2$Cl$_2$ (73.54(5)°, 79.633(17)°) can be compared with the sulphur analogue, [Pt(SC$_4$H$_3$N$_2$)$_2$(dppm)] (73.73(3)°; S–Pt–S = 79.35(3)°) [13] and [Pt(SC$_5$H$_4$N)$_2$(dppm)] (74.01(4)°; S–Pt–S = 78.56(4)°) [12].

3.3. Theoretical study

X-ray structural analyses for several dichalcogenolate complexes show subtle differences in the conformations. However such differences could not be diagnosed in solution even for the complexes containing bulky aryl groups like mesityl. To understand possible reasons for observed conformational variations, DFT calculations were performed. Three minimum energy structures are obtained in each of these three (S, Se or Te based mesityl chalcogenolate with dppp as a co-ligand) cases with various possible input structures for the three complexes based on different spatial orientations of the ligands. Optimization of structures are carried out applying a DFT functional, namely, BP86 which is known to work well for platinum based complexes considering mixed atomic basis functions. The optimized structures look similar and the final optimized structures are displayed in Fig. 5. In case of thiolate and selenolate complexes, conformers **IA** and **IIA** (where mesityl rings

Table 6
Selected bond lengths (Å) and angles (°) of [Pt{SeC$_5$H(4,6-Me)N$_2$}$_2$(dppm)]·CH$_2$Cl$_2$.

Pt1–P1	2.2550(12)	Pt1–P2	2.2523(13)
Pt1–Se1	2.4568(6)	Pt1–Se2	2.4445(5)
Se1–C26	1.910(5)	Se2–C32	1.908(5)
P1–Pt1–P2	73.54(5)	Se1–Pt1–Se2	79.633(17)
P1–Pt1–Se1	102.85(3)	P2–Pt1–Se1	175.81(4)
P1–Pt1–Se2	174.99(4)	P2–Pt1–Se2	104.14(3)
C26–Se1–Pt1	111.96(15)	C32–Se2–Pt1	113.64(14)
P1–Pt1–Se1–C26	17.10(17)	P2–Pt1–Se1–C26	47.0(5)
P1–Pt1–Se2–C32	64.3(4)	P2–Pt1–Se2–C32	2.48(17)
C26–Se1–Pt1–Se2	−158.45(16)	C32–Se2–Pt1–Se1	−175.66(16)

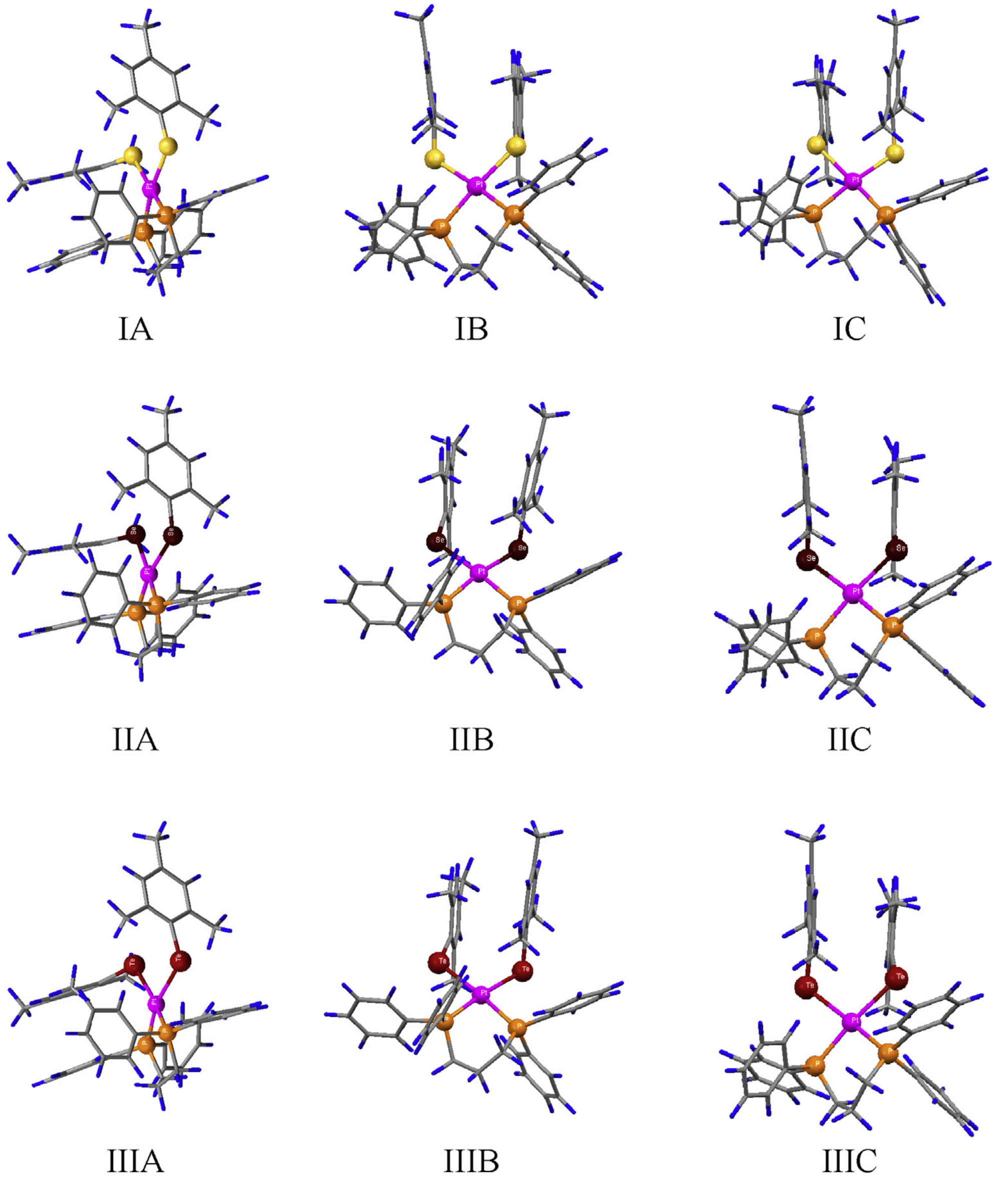

Fig. 5. Optimized structures of different conformers of S, Se and Te based mesitylchalcogenolate (I: S, II: Se and III: Te) complexes of platinum calculated at DFT level of theory.

on chalcogen ligands are mutually perpendicular) are the most stable ones. For tellurolate, **IIIB** conformer (mesityl rings are parallel to each other) is the most stable one. However, the energy difference (ΔE) is very small between conformers **A** and **B** in all the three cases. For thiolate, selenolate and tellurolate complexes ΔE between **A** and **B** conformers and that between **A** and **C** conformers is calculated to be 0.1, 0.5 and 1.0 kcal/mol and 1.0, 2.2 and 3.1 kcal/mol, respectively. Calculated geometrical parameters of the most stable conformer are very close to that of the X-ray data (for selenolate and tellurolate complexes). In each minimum energy structure, a pair of aryl rings (unsubstituted–substituted or substituted–substituted) is observed to be stacked in parallel fashion allowing π–π interaction between aryl rings to provide extra stability for the observed conformer of the complexes.

4. Conclusions

The relative orientation of the aryl groups attached to the chalcogen atom is a distinguishing feature among the several structures reported here and in the literature. The observed orientation of the aryl group in the solid state may possibly due to subtle crystal energy packing requirement. The DFT calculations suggest that there is a very small energy difference among various conformers which make them indistinguishable in solution.

Acknowledgements

One of the authors (RSC) is grateful to DAE for the award of SRF. We thank Drs. T. Mukherjee and D. Das for encouragement of this work.

Appendix A. Supplementary material

CCDC 916604 (for [Pt(SeMes)$_2$(dppp)]·½C$_6$H$_6$), CCDC 916607 (for [Pt(TeMes)$_2$(dppp)]·3C$_6$H$_6$), and 916606 (for [Pt{SeC$_4$H(4,6-Me$_2$)N$_2$}$_2$(dppm)]·CH$_2$Cl$_2$) contain the supplementary crystallographic data for this paper. These data can be obtained free of charge from The Cambridge Crystallographic Data Centre via www.ccdc.cam.ac.uk/data_request/cif.

Appendix B. Supplementary material

Supplementary data associated with this article can be found in the online version, at http://dx.doi.org/10.1016/j.jorganchem.2013.03.030.

References

[1] V.K. Jain, L. Jain, Coord. Chem. Rev. 254 (2010) 2848–2903.
[2] A. Singhal, V.K. Jain, A. Klein, M. Niemeyer, W. Kaim, Inorg. Chim. Acta 357 (2004) 2134–2142.
[3] J. Fornies-Camer, A.M. Masdeu-Bulto, C. Claver, Inorg. Chem. Commun. 5 (2002) 351–354.
[4] I.P. Beletskaya, V.P. Ananikov, Pure Appl. Chem. 79 (2007) 1041–1056.
[5] V.P. Ananikov, I.P. Beletskaya, G.G. Aleksandrov, I.L. Eremenko, Organometallics 22 (2003) 1414–1421.
[6] M.S. Hannu-Kuure, J. Komulainen, R. Oilunkanieme, R.S. Laitinen, R. Suontamo, M. Ahlgren, J. Organomet. Chem. 666 (2003) 111–120.
[7] R.D. Lai, A. Shaver, Inorg. Chem. 20 (1981) 477–480.
[8] V.K. Jain, S. Kannan, R.J. Butcher, J.P. Jasinski, J. Chem. Soc., Dalton Trans. (1993) 1509–1513.
[9] A. Singhal, V.K. Jain, B. Varghese, E.R.T. Tiekink, Inorg. Chim. Acta 285 (1999) 190–196.
[10] A.K. Fazlur-Rahman, J.G. Verkade, Inorg. Chem. 31 (1992) 5331–5335.
[11] M.K. Pal, V.K. Jain, A. Wadawale, S.A. Glazun, Z.A. Starikova, V.I. Bregadze, J. Organomet. Chem. 696 (2010) 4257–4263.
[12] A. Mendia, E. Cerrada, F.J. Arnaiz, M. Laguna, Dalton Trans. (2006) 609–616.
[13] T.S. Lobana, P. Kaur, G. Hundal, R.J. Butcher, A. Castineiras, Z. Anorg. Allg. Chem. 634 (2008) 747–753.
[14] S. Narayan, V.K. Jain, B. Varghese, J. Chem. Soc., Dalton Trans. (1998) 2359–2366.
[15] R.S. Chauhan, G. Kedarnath, A. Wadawale, A.L. Rheingold, A. Munoz-Castro, R. Arratia-Perez, V.K. Jain, Organometallics 31 (2012) 1743–1750.
[16] R.S. Chauhan, R.K. Sahrma, G. Kedarnath, D.B. Cordes, A.M.Z. Slawin, V.K. Jain, J. Organomet. Chem. 717 (2012) 180–186.
[17] T.G. Appleton, M.A. Bennett, I.B. Tomkins, J. Chem. Soc., Dalton Trans. (1976) 439–446.
[18] M. Bochmann, K.J. Webb, M.B. Hursthouse, M. Mazid, J. Chem. Soc., Dalton Trans. (1991) 2317–2323.
[19] M. Akiba, M.V. Lakshmikantham, K.Y. Jen, M.P. Cava, J. Org. Chem. 49 (1984) 4819–4821.
[20] N.D. Ghavale, S. Dey, V.K. Jain, M. Netaji, Inorg. Chim. Acta 361 (2008) 2462–2470.
[21] G.M. Sheldrick, Acta Crystallogr. A64 (2008) 112–122.
[22] C.K. Johnson, ORTEP II, Report ORNL-5136, Oak Ridge National Laboratory, Oak Ridge, TN, 1976.
[23] K.L. Schuchardt, B.T. Didier, T. Elsethagen, L. Sun, V. Gurumoorthi, J. Chase, J. Li, T.L. Windus, J. Chem. Inf. Model. 47 (2007) 1045–1052.
[24] M.W. Schmidt, K.K. Baldridge, J.A. Boatz, S.T. Elbert, M.S. Gordon, J.H. Jensen, S. Koseki, N. Matsunaga, K.A. Nguyen, S.J. Su, T.L. Windus, M. Dupuis, J.A. Montgomery, J. Comput. Chem. 14 (1993) 1347–1363.
[25] P.E. Garrou, Chem. Rev. 81 (1981) 229–266.
[26] W.E. Hill, D.M.A. Minahan, G.G. Taylor, C.A. McAuliffe, J. Am. Chem. Soc. 104 (1982) 6001–6005.
[27] N.K. Lokanath, H.C. Devarajegowda, S.M. Anadalwar, J.S. Prasad, S. Narayan, V.K. Jain, Anal. Sci. 17 (2001) 565–566.
[28] M. Risto, E.M. Jahr, M.S. Hannu-Kurre, R. Oilunkaniemi, R.S. Laitinen, J. Organomet. Chem. 692 (2007) 2193–2204.